International Immunology, Vol. 29, No. 5, pp. 211–220
doi:10.1093/intimm/dxx032
Advance Access publication 24 May 2017

Integrity of immunoglobulin variable regions is supported by GANP during AID-induced somatic hypermutation in germinal center B cells

Mohammed Mansour Abbas Eid[1]*, Mayuko Shimoda[2–4]*, Shailendra Kumar Singh[3], Sarah Ameen Almofty[5], Phuong Pham[6], Myron F. Goodman[6], Kazuhiko Maeda[3,4] and **Nobuo Sakaguchi[7,8]**

[1]Clinical Pathology Department, Faculty of Medicine, Fayoum University, PO Box 63514, Fayoum, Egypt
[2]Department of Immunology, Graduate School of Medical Sciences, Kumamoto University, 1-1-1 Honjo, Kumamoto 860-8556, Japan
[3]Laboratory of Host Defense, World Premier International Research Center Initiative (WPI) Immunology Frontier Research Center (IFReC) and
[4]Department of Host Defense, Research Institute for Microbial Diseases (RIMD), Osaka University, 3-1 Yamada-oka, Suita, Osaka 565-0871, Japan
[5]Laboratory of Immunology, Institute for Research and Medical Consultations (IRMC), University Of Dammam (UOD), PO Box 1982, Dammam 31441, Saudi Arabia
[6]Departments of Biological Sciences and Chemistry, University of Southern California, 1050 Childs Way, University Park, Los Angeles, CA 90089-2910, USA
[7]World Premier International Research Center Initiative (WPI) Immunology Frontier Research Center, Osaka University, 3-1 Yamada-oka, Suita, Osaka 565-0871, Japan
[8]Tokyo Metropolitan Institute of Medical Science, 2-1-6, Kamikitazawa, Setagaya-ku, Tokyo 156-8506, Japan

Correspondence to: K. Maeda; E-mail: kazmaeda@biken.osaka-u.ac.jp

*These authors contributed equally to this work.

Received 27 March 2017, *editorial decision* 19 May 2017; *accepted* 22 May 2017

Abstract

Immunoglobulin affinity maturation depends on somatic hypermutation (SHM) in immunoglobulin variable (IgV) regions initiated by activation-induced cytidine deaminase (AID). AID induces transition mutations by C→U deamination on both strands, causing C:G→T:A. Error-prone repairs of U by base excision and mismatch repairs (MMRs) create transversion mutations at C/G and mutations at A/T sites. In Neuberger's model, it remained to be clarified how transition/transversion repair is regulated. We investigate the role of AID-interacting GANP (germinal center-associated nuclear protein) in the IgV SHM profile. GANP enhances transition mutation of the non-transcribed strand G and reduces mutation at A, restricted to GYW of the AID hotspot motif. It reduces DNA polymerase η hotspot mutations associated with MMRs followed by uracil-DNA glycosylase. Mutation comparison between IgV complementary and framework regions (FWRs) by Bayesian statistical estimation demonstrates that GANP supports the preservation of IgV FWR genomic sequences. GANP works to maintain antibody structure by reducing drastic changes in the IgV FWR in affinity maturation.

Keywords: activation-induced cytidine deaminase, affinity maturation, antibody, DNA repair pathways, SHM

Introduction

Naive B cells expressing BCRs of the primary repertoire specifically recognize various exogenous antigens and undergo affinity maturation for acquired immunity during their proliferation in the germinal centers (GCs) of lymphoid follicles. The immunoglobulin variable (IgV) region undergoes diversification in antigen-driven B cells with somatic hypermutation (SHM) initiated by activation-induced cytidine deaminase (AID) (1–3), followed by subsequent selection of high-affinity B cells in the GCs (4–6). AID induces C→U deamination, preferentially at WRC (W = A or T, R = A or G) hotspot motifs on both the template and non-template strands of the rearranged IgV region during active transcription (4, 7–10). Studies of SHM in

the IgV region by Neuberger's group using uracil-DNA glycosylase (UNG) and mismatch repair (MMR)-deficient mice suggested a two-phase stepwise model by which AID-generated U is processed in the IgV region (11, 12). In this model, B cells undergo another round of cell division, creating C→T and G→A transition (Ts) mutations by direct replication opposite U-containing templates (Phase 1a). The removal of U by UNG and replication across the resulting abasic sites during base excision repair (BER) generates C→(G/A) and G→(C/T) transversions (Tv) in addition to Ts mutations (Phase 1b). Further SHM diversification involves error-prone MMR, during which the short patches of DNA sequences surrounding U:G mismatches are excised and inaccurately resynthesized by error-prone DNA polymerases concurrently expressed in GC B cells (Phase 2) (13–19). Phase 2 of SHM gives rise to a variety of mutations, including A→(T/G/C) and T→(C/G/A), in the DNA regions surrounding the G:U mismatch. Thus, sites of AID-induced cytidine deamination might represent special anchoring sites from which SHM mutations spread throughout the rearranged IgV regions.

AID initiates both IgV-region SHM and switch-region (S-region) class switch recombination (CSR) (13, 20, 21). The level of AID-induced mutation at the S-region sequences exclusively correlates with the rate of CSR. However, in the case of affinity maturation, the overall rate of IgV region seems not to correlate with the increase in the antibody affinity for the target antigen. The generation of high-affinity antibodies depends not only on IgV-region SHM, but also on the antigen-driven selection process. Analyses of IgV-region SHM and the selection process have shown the importance of the SHM mutation types and their distributions across the IgV regions for the production of high-affinity memory and plasma B cells (22, 23). High-throughput IgV sequencing and computational methods have been used to study the antigen-driven selection process during the affinity maturation of human IgV (24–26). In particular, Yaari *et al.* (27) developed a Bayesian statistical method, 'BASELINe', to detect and quantify the selection work by comparing the observed frequencies of non-synonymous amino acid replacement (R) mutations and silent synonymous (S) mutations with the expected frequencies for R and S. The expected frequencies for R and S are calculated based on the underlying targeting model to account for SHM hot and cold spots and any nucleotide substitution bias (27, 28). This approach has demonstrated different selection pressures acting on the IgV complementarity-determining regions (CDRs) and the framework regions (FWRs) during the maturation of antigen-driven B cells in the peripheral lymphoid organs. Hershberg and Shlomchik (5), who focused on the mutation profile and the codon usage of the genomic IgV-region sequences, noted the differences in potential of amino acid changes in the IgV-region CDRs and FWRs of the heavy and light chains. Thus, a simple random increase in IgV-region SHM does not directly correlate with the affinity maturation of antigen-specific B cells, but the types of SHM mutations leading to advantageous amino acid changes in individual IgV regions are important for the generation of high-affinity B cells.

GANP (germinal center-associated nuclear protein) is required for the affinity maturation of antigen-specific B cells in the mouse system after immunization with T-cell-dependent antigens (29, 30). B-cell-specific *Ganp*-deficient (B-GANP$^{-/-}$) mice showed impairment in their affinity maturation of antibodies against immunizing antigens. In contrast, B-cell-specific *Ganp*-transgenic (GANP^{Tg}) mice generate much higher affinity antibodies for antigens such as 4-hydroxy-3-nitrophenylacetyl (NP)–hapten and the HIV 1 gp41 epitope (31). GANP is involved in the IgV transcription complex after shepherding AID toward the nucleus to allow AID access (32) and regulates nucleosome occupancy for transcription in the rearranged IgV region (33). While GANP markedly increases the access of AID to IgV-region loci, its effect on the SHM mutation rate in the antigen-specific high-affinity hybridomas remains modest. Here, we studied the effect of GANP on the SHM profile in the levels of nucleotide and amino acid of IgV-region CDRs and FWRs in generation of antigen-specific high-affinity B cells.

Methods

BASELINe program analysis

Mutated sequences were prepared in the FASTA format and aligned using the Clustal Omega multiple sequence alignment tool (http://www.ebi.ac.uk/Tools/msa/clustalo/). The sequences were prepared according to the software guidelines and uploaded to the server (27, 28). Briefly, the sequences were aligned so that the V_H186.2 germline was the first sequence. The V_H186.2 germline sequence was used as the 'consensus' sequence to which all the other sequences were compared. The identified mutations were classified as either silent (S) or replacement (R) mutations.

Protein Variability Server

The protein sequences were extracted from the original base sequence data using EMBOSS Transeq (http://www.ebi.ac.uk/Tools/st/emboss_transeq/). The sequences were prepared in the FASTA format and aligned as described above. The aligned sequences were analyzed for protein variability using the Protein Variability Server (PVS) implementing Shannon entropy (34) (http://imed.med.ucm.es/PVS).

Isolation of GC B cells

B-cell-specific GANP^{Tg} and B-GANP$^{-/-}$ mice have been described previously (32, 33). The mice were immunized with NP–chicken γ-globulin (NP–CGG) in alum (100 μg per mouse) for 14 days and their splenic B cells were isolated with a B-cell isolation kit combined with a magnetic cell sorter (autoMACS Pro Separator; Miltenyi Biotec). The GC B cells were isolated from the B220^{+}GL-7^{+}Fas^{+} population with a FACSAria cell sorter (BD Biosciences). All animal experiments were performed with approval from the Center for Animal Resources and Development of Kumamoto University Animal Care and Use Committee and the Animal Research Committee of the Research Institute for Microbial Diseases of Osaka University.

IgV-region sequence and SHM

The IgV-region sequences from the immunized mice were analyzed with PCR using primer pair of the forward 5′-TTCTTGGCAGCAACAGCTACAGGTAAGG-3′ and the reverse 5′-GCAGGCTTGAGGTCTGGACATATACATG-3′. The aligned sequences of IgV region were analyzed for mutation patterns using SHMTool, as previously described (35).

The AID-bound IgV-region sequences from Ramos transfectants were analyzed with PCR using primer pair of the forward 5′-TGGGGCGCAGGACTGTTGAAGCCTTC-3′ and the reverse 5′-CCTTGGCCCCAGACGTCCAT-3′.

Measurement of UNG activity

A 33-nt oligonucleotide (5′-AAAGTGGAAAG**U**AAAGAGGAAA GGTGAGGAGGT-3′) was 5′-end labeled with ^{32}P using T4 polynucleotide kinase. The labeled oligonucleotide was annealed to a complementary strand to form a dsDNA substrate containing a G:U mismatch. The nuclear extract from cells of the human B-cell line Ramos were prepared as described previously (33). The uracil excision activity in the Ramos cell extract was measured by incubating 250 fmol of the ^{32}P-labeled dsDNA with 200 ng of the nuclear extract in a buffer containing 10 mM Tris–HCl (pH 8), 1 mM dithiothreitol, and 1 mM EDTA (30 μl volume). When appropriate 6 μof an anti-SMUG1 neutralizing antibody (36) was pre-incubated with the Ramos nuclear extract for 3 min at 37°C before the addition of the DNA substrate. After incubation for 1–20 min, the reactions were quenched by double extraction with phenol:chloroform:isoamyl alcohol (25:24:1). To cleave the abasic site that resulted from the excision of U, the reaction mixtures were heated at 95°C for 5 min in the presence of 0.1 N NaOH. The cleaved product (11 nt) and uncleaved substrate (33 nt) were separated on a 16% denaturing PAGE gel, visualized and quantified with a STORM phosphorimager scanner and the ImageQuant software (GE Healthcare). The specific activity of the enzyme, defined as femtomole of excised U per minute per milligram of cell extract, was measured in the linear range of the cell extract concentration against time, after incubation for 5 or 10 min.

Results

Antigen-driven IgV-region profile of GC B cells from GANP mutant mice

We have previously shown that GANP^{Tg} mice generate antibodies with much higher affinity for NP–CGG than those produced by wild-type (WT) mice (31). To further understand the mechanism of the GANP-mediated increase in antibody affinity, we investigated the effect of GANP on the IgV-region SHM profile in mouse GC B cells after immunization with NP–CGG. Mice were immunized with NP–CGG for 14 days and the GC B cells expressing B220$^+$GL-7$^+$Fas$^+$ were purified with cell sorting. Sequence analysis of the V_H186.2 region showed that the mutation frequency was significantly lower in the B-GANP$^{-/-}$ mice than in the GANP$^{F/F}$ mice (Fig. 1a; Supplementary Table S1, available at *International Immunology* Online). On the contrary, we found an alteration in the SHM profile of the GANP^{Tg} mice, with a significant increase in the proportion of Ts mutations at C/G sites (Fig. 1b, V_H186.2; Supplementary Figure S1, available at *International Immunology* Online) and a significant reduction in mutations at A/T sites (Fig. 1c, V_H186.2; Supplementary Figure S1, available at *International Immunology* Online), suggesting that the GANP overexpression affected the SHM mutation types and their distribution in the IgV region in GC B cells.

We employed the BASELINe program to compare the IgV-region SHM profiles and antigen-driven selection with 50 sequences of the V_H186.2 region from each B-cell group by analyzing through five steps (27, 28):

1. SHM point mutations were grouped by location (CDRs or FWRs) and type [replacement (R) or silent (S)]. The observed and expected numbers of mutations were then calculated for each category.
2. A posterior probability distribution function (PDF) was calculated for the Bayesian estimation of the R frequency for each sequence.
3. Germline normalization allowed the direct comparison of sequences with different R frequencies. In this step, an estimate of the selection strength (Σ) for each sequence was calculated. Positive (negative) values for Σ arise when the estimated R-to-S frequency is higher (lower) than expected, indicating positive (negative) selection.
4. The results for multiple sequences were combined to calculate a single PDF for Σ for each group of sequences.
5. Selection was determined and Σ was compared between groups. The BASELINe analysis of the immunoglobulin sequences spanning the V and J regions of each group of mice is shown in Fig. 2(a) in the form of PDFs of the estimated Σ values in the CDR and FWR.

The results show significant positive selection in the CDR (Fig. 2a, red line and red dashed line) with the mean Σ estimated to be 0.38–1.2 for all four groups of mice. In contrast, there was clear negative selection in the FWR, with a mean Σ ranging from −0.25 to −0.75 (Fig. 2a, blue line and blue dashed line). Compared with the WT mice (lines), the GANP^{Tg} mice had lower positive Σ in the CDR (red dashed line) (mean Σ = 0.525 for GANP^{Tg} versus 0.724 for WT) and had a more negative Σ in the FWR (blue dashed line) (mean Σ = −0.668 for GANP^{Tg} versus −0.319 for WT) (Fig. 2a, right panel). The B-GANP$^{-/-}$ mice showed no obvious change in the strength of the positive selection in the CDR (red dashed line). In contrast, the B-GANP$^{-/-}$ mice displayed a slightly more negative Σ value in the FWR (blue dashed line) compared with the GANP$^{F/F}$ (blue solid line) (Fig. 2a, left panel). However, this could be explained by the markedly reduced mutation in the absence of GANP, leading to a considerable reduction in amino acid substitutions, especially in FWR3 (Fig. 2b). Alternatively, GANP may not be the sole player maintaining the negative selection in the FWRs. Taking these findings together, the expression of GANP may promote stronger negative selection for maintaining the specificity and stable three-dimensional structures of antibodies.

Effect of GANP expression on the IgV-region SHM profile in the Ramos B-cell line

To investigate the primary effect of GANP on the IgV-region SHM profile, we used the Ramos B-cell line maintained *in vitro*. The IgV-region SHM profiles of Ramos B cells overexpressing (O/E) GFP-tagged GANP (GANP$^{O/E}$) or GFP alone (GFP$^{O/E}$) were re-analyzed with slight modification (32). We obtained the re-analyzed IgV-region sequences from AID-immunoprecipitation (AID-IP) to give a more accurate picture of SHM between GFP$^{O/E}$ and GANP$^{O/E}$, which were not obtained in the previous condition. The GFP$^{O/E}$ cells showed the mutation pattern of C→T (4%) and G→A (4%) in the genomic IgV

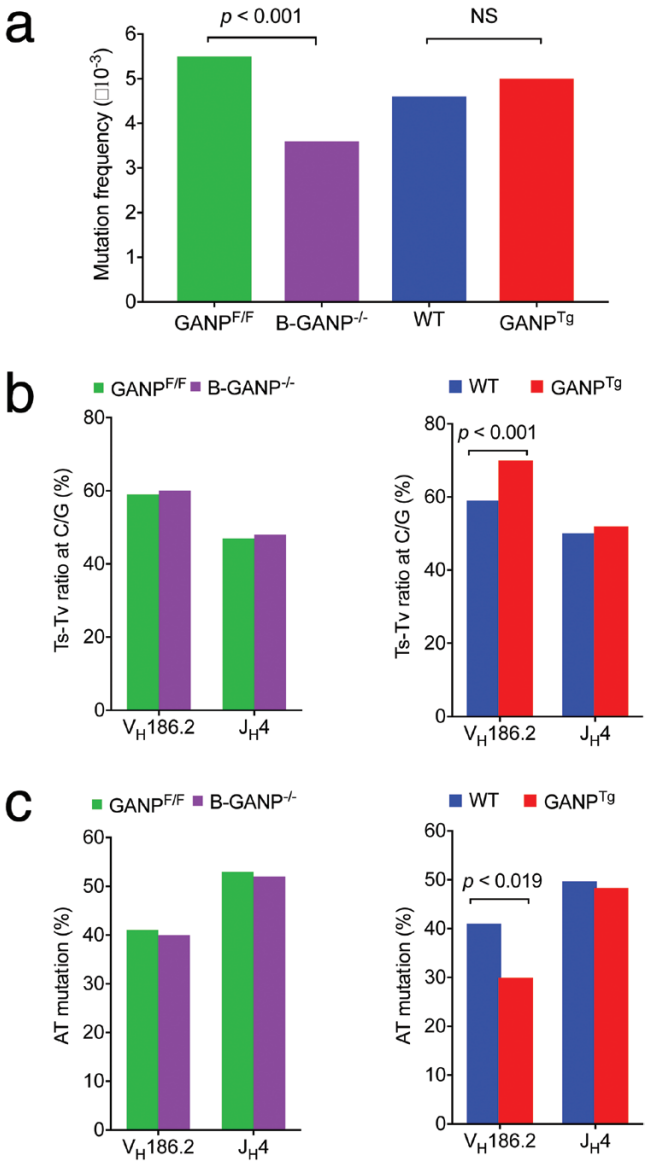

Fig. 1. Mutation frequency in GANP mutant mice. (a) Overall mutation frequencies in GANP mutant mice. (b) Mutation bias in GANP mutant mice. Data are the Ts:Tv ratios at C/G sites (%) in the V_H186.2 and J_H4 regions. (c) A/T mutation bias in GANP mutant mice. Data are the AT mutation (%) in the V_H186.2 and J_H4 regions. The graphs are drawn from the data in Supplementary Table S1 (available at *International Immunology* Online).

region (Fig. 3a, left upper panel), whereas GANP$^{O/E}$ altered the mutation pattern to C→T (35%) and G→A (35%) (Fig. 3a, left lower panel). This Ts bias is similar to that observed in the AID-bound IgV-region sequences (Fig. 3a, right panel). The AID-bound IgV region showed predominantly Ts mutations occurring at G/C template bases, G→A (32%) and C→T (13%) in GFP$^{O/E}$ cells and G→A (37%) and C→T (27%) in GANP$^{O/E}$ cells (Fig. 3a, right panel). Mutations at A/T template bases represented only 10 and 5% of mutations in GANP$^{O/E}$ and GFP$^{O/E}$, respectively.

GANP overexpression in Ramos cells led to an ~2-fold increase in the IgV-region SHM mutation frequency (1.72×10^{-3} for GANP$^{O/E}$ versus 0.85×10^{-3} for GFP$^{O/E}$) (Fig. 3b, left panel). The genomic IgV sequences from GANP$^{O/E}$ cells contained an increased ratio of C/G versus A/T mutations (86:14 = 6.1) compared with that of GFP$^{O/E}$ cells (43:57 = 0.75). In particular, the Ts:Tv ratio at the C/G sites was markedly increased in the GANP$^{O/E}$ cells (82:18 = 4.6 for GANP$^{O/E}$ cells versus 20:80 = 0.24 for GFP$^{O/E}$ cells) (Fig. 3b). In the AID-bound IgV region, we observed a similar ~2-fold increase in the SHM frequency in the GANP$^{O/E}$ cells, and a significant increase in the Ts:Tv ratio at the C/G sites in the GANP$^{O/E}$ cells (62:38 = 1.6 versus 38:62 = 0.6 for GFP$^{O/E}$ cells) (Fig. 3b, right panel). The Ts:Tv ratio at the A/T sites appeared to be the same for the GANP$^{O/E}$ and GFP$^{O/E}$ cells. For both the genomic IgV and AID-bound IgV sequences, SHM mutations occurred at C sites much more frequently in GANP$^{O/E}$ cells than in GFP$^{O/E}$ cells (see the C:G ratio in Fig. 3b). These data suggest that the overexpression of GANP in Ramos B cells greatly increased the Ts mutations at C/G sites.

Association of amino acid changes with IgV affinity maturation

It has been shown that IgV sequences have evolved to tolerate extensive cytidine deamination (37). To maximize affinity maturation, C and G bases are often precisely positioned in codons so that C→T and G→A mutations cause silent or conservative amino acid changes (37). Because the IgV-region SHM profile is biased toward Ts mutations at C/G sites in GANP$^{O/E}$ GC B cells, we examined the effect of GANP on the pattern of amino acid replacement in the selected IgV region. The relationship between the SHM of V_H186.2 sequences and antibody affinity was evaluated by examining hybridomas that secrete high-affinity anti-NP monoclonal antibodies. The monoclonal antibodies from GANP^{Tg} and WT mice, which displayed similar high affinity (K_D < 1 × 10^{-7} M) for the NP–hapten, were compared from our previous report (31). Overall, the number of mutations in the V regions of monoclonal antibodies appeared to correlate inversely with the K_D value, indicating that monoclonal antibodies with a higher number of SHMs have higher affinity for the antigen (Supplementary Figure S2, available at *International Immunology* Online). Importantly, when we compared the monoclonal antibody amino acid sequences in detail using a strategy that classified amino acid mutations into groups with similar ('change replacement') or different ('trait replacement') properties of hydrophobicity, polarity and size (5), we found that amino acid changes occurred preferentially within the same groups in the GANP^{Tg} mice (change 21/30 = 70%) but did not in the WT mice (13/30 = 43%) (Supplementary Table S2, available at *International Immunology* Online). When we considered the amino acid mutation distribution in the IgV structure, the CDRs of the monoclonal antibodies from the GANP^{Tg} mice showed 89% preference for amino acid change replacements with the same properties, compared with 47% in the WT mice (Supplementary Table S2, available at *International Immunology* Online). The FWRs showed fewer amino acid trait replacements in the monoclonal antibodies from the GANP^{Tg} mice (64%) than did those in the monoclonal antibodies from WT mice (71%) (Supplementary Table S2, available at *International Immunology* Online).

We further analyzed the sites of IgV-region SHM and the amino acid mutations in antigen-reactive B cells undergoing IgV-region SHM in the GCs of the GANP^{Tg} and WT

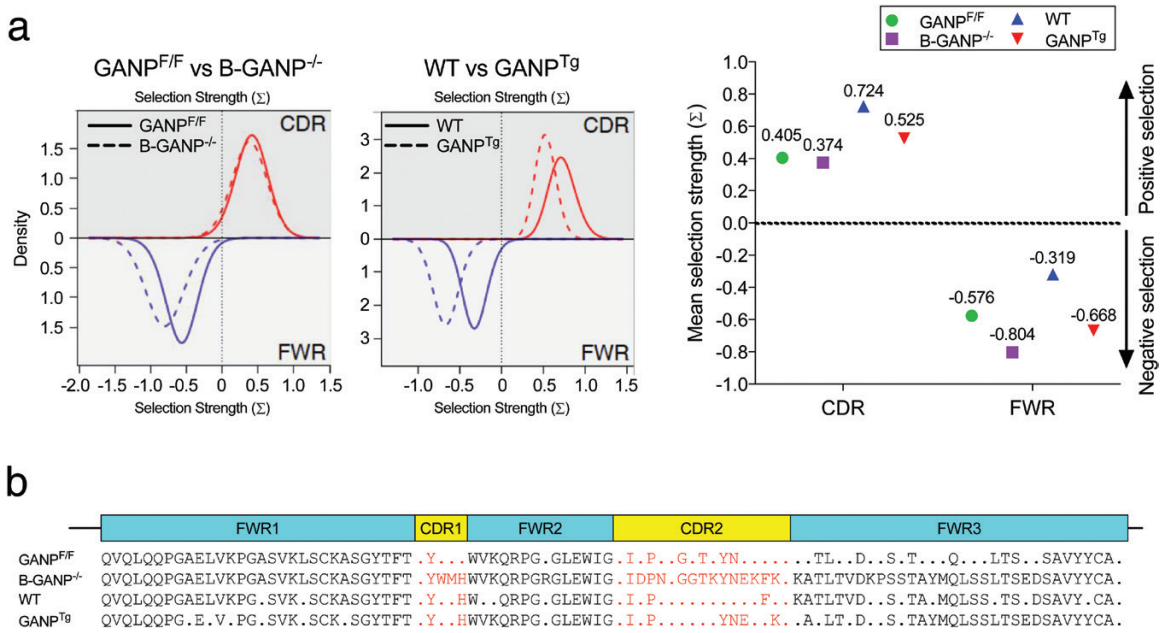

Fig. 2. Bayesian estimation of antigen-driven selection in the sequences of the V_H186.2 region in NP-CCG immunized GANP mutant mice. (a) The left graphs display the posterior PDF for the immunoglobulin sequences from the GANP$^{F/F}$ (continuous line) and B-GANP$^{-/-}$ (dotted line) and from WT (continuous line) and GANP^{Tg} (dotted line), respectively. The top half of each plot shows the estimated selection strength in the CDR, and the bottom part provides an estimate for the FWR (27). The right side graph shows the value of mean selection strength (Σ) among GANP mutant mice for CDR and FWR of V_H186.2 region. (b) Protein variability plot (34). Sequence variability is plotted against the consensus sequence, used as the reference sequence. Protein variability is measured as Shannon entropy, according to PVS guidelines (http://imed.med.ucm.es/PVS). Dots represent variable positions, i.e. amino acid positions subject to variation caused by SHM.

mice. The frequency of hotspot usage (GYW) for AID cytidine deamination was markedly increased in the GANP^{Tg} GC B cells relative to those from the WT mice (from 25 to 38%), whereas only a few were altered in the GC B cells of the B-GANP$^{-/-}$ mice (Fig. 4a). Amino acid mutations in V_H186.2 were more frequently amino acid change replacements (282/424 = 67%) in the GANP^{Tg} mice than in the WT mice (259/427 = 61%) in both the CDRs and FWRs (Fig. 4b; Supplementary Table S3, available at *International Immunology* Online). This conservative bias toward amino acid change replacement was slightly elevated in GANP^{Tg} mice compared with WT mice in both the CDRs (63 versus 59%, respectively) and FWRs (71 versus 62%, respectively). Remarkably, the amino acid mutations in the B-GANP$^{-/-}$ mice showed the opposite patterns to those observed in the GANP^{Tg} mice. Compared with the GANP$^{F/F}$, the B-GANP$^{-/-}$ mice displayed more non-conservative amino acid trait replacements (24 versus 47%, respectively) for the whole IgV region, and significantly more amino acid trait replacements in the FWRs (26 versus 80%, respectively) (Fig. 4a; Supplementary Table S3, available at *International Immunology* Online). Concurrently, conservative amino acid change replacements in V_H186.2 occurred at a lower frequency in the B-GANP$^{-/-}$ mice than in the GANP$^{F/F}$ mice (53 versus 76%, respectively), and a reduction in the amino acid change replacements was also observed in both the CDRs (76 versus 81%, respectively) and FWRs (20 versus 74%, respectively). Therefore, GANP expression in B cells appears to protect them from amino acid trait replacements in the IgV region, especially in the FWRs. This result indicates the critically important role of GANP in the preservation of the three-dimensional antibody structure.

Effects of GANP on IgV-region SHM mutations at A/T sites in DT40 cells

GANP skews the SHM profile towards Ts mutations at C/G sites, accompanied by a reduction in the C/G Tv mutations and a reduction in mutations at A/T sites (Figs 1 and 3; Supplementary Figure S1, available at *International Immunology* Online). These changes in the SHM profile are quite similar to those reported previously in the B cells of UNG$^{-/-}$ mice (13) and in chicken DT40 B cells (38). Therefore, we re-examined the effects of GANP on the SHM profile in the genomic IgV_L segment of DT40 B cells (Supplementary Figure S3a, available at *International Immunology* Online) (39). We used an UNG$^{-/-}$ mutant DT40 clone that does not undergo gene conversion in the IgV region, but instead produces SHM Ts mutations in the IgV region upon the introduction of AID (AID^{R}UNG$^{-/-}$) (39). GANP$^{O/E}$ in AID^{R}UNG$^{-/-}$ cells induces a marked 7-fold increase in the SHM mutation frequency (105.5×10^{-3}) compared with that in the AID^{R}UNG$^{-/-}$ cells (14.5×10^{-3}) (Supplementary Figure S3b, available at *International Immunology* Online). Interestingly, the GANP$^{O/E}$ in AID^{R}UNG$^{-/-}$ cells showed a dramatic shift in the IgV_L SHM profile, with nearly 100% of mutations occurring at C/G sites and almost all Ts mutations. Although the AID^{R}UNG$^{-/-}$ Mock control cells also predominantly contained Ts mutation at C/G sites, we still observed a substantial number of SHM mutations at A/T sites (9.2% A→G/T and 19.8% T→C/G). The GANP-mediated inhibition of SHM mutations at A/T sites in

a

Genomic IgV-region

From	To A	C	G	T	%
GFP$^{O/E}$ A	*	57	0	0	57
GFP$^{O/E}$ C	0	*	0	4	4
GFP$^{O/E}$ G	4	0	*	35	39
GFP$^{O/E}$ T	0	0	0	*	0
	A	C	G	T	
GANP$^{O/E}$ A	*	12	2	0	14
GANP$^{O/E}$ C	0	*	6	35	41
GANP$^{O/E}$ G	35	2	*	8	45
GANP$^{O/E}$ T	0	0	0	*	0

AID-IP IgV-region

From	To A	C	G	T	%
GFP$^{O/E}$ A	*	2.5	2.5	0	5
GFP$^{O/E}$ C	0	*	13	13	26
GFP$^{O/E}$ G	32	27	*	10	69
GFP$^{O/E}$ T	0	0	0	*	0
	A	C	G	T	
GANP$^{O/E}$ A	*	2	4	0	6
GANP$^{O/E}$ C	4	*	9	27	40
GANP$^{O/E}$ G	37	11	*	2	50
GANP$^{O/E}$ T	2	1	1	*	4

b

	Ramos		AID-IP	
	GFP$^{O/E}$	GANP$^{O/E}$	GFP$^{O/E}$	GANP$^{O/E}$
Mutation freq. ($\times 10^{-3}$)	0.85	1.72	2.2	4.0
CG : AT	43 : 57	86 : 14	95 : 5	90 : 10
Ts/Tv	8 : 92	72 : 38	47.5 : 52.5	69 : 31
Ts : Tv at C/G	20 : 80	82 : 18	38 : 62	62 : 38
Ts : Tv at A/T	0 : 100	14 : 86	50 : 50	44 : 56
C/G ratio	0.1	0.9	0.4	0.8

Fig. 3. GANP-mediated mutations in the rearranged IgV region in human Ramos B cells. (a) Mutations in the rearranged V-region segment from genomic DNA (left) and after AID-IP (right) from GFP$^{O/E}$ and GANP$^{O/E}$ Ramos cells. The genomic IgV sequences were re-analyzed from previously published clones (32), and the AID-bound IgV sequences were newly obtained. Patterns of nucleotide substitutions are expressed as the percentages of the total mutations after correction for base composition. (b) The ratio of the mutations at C/G to those at A/T is indicated, as is the ratio of Ts:Tv substitutions at both C/G and A/T. The ratio of total Ts to total Tv and the C:G ratio are also shown.

DT40 B cells suggests that GANP is involved in regulation of error-prone MMR and/or access of polymerase η to the IgV region, which are principally responsible for SHM at A/T sites.

Effect of GANP on UNG activity

The effect of GANP on UNG activity was examined with an *in vitro* assay using a ^{32}P-labeled 33-bp heteroduplex DNA substrate carrying a single U:G mismatch. The substrate DNA was incubated with Ramos B-cell nuclear extract and treated mildly with sodium hydroxide to cleave the abasic site. It was resolved with denaturing PAGE and visualized with phosphorimaging (Fig. 5). Only the 33-nt DNA substrate was detectable in the absence of cell extract (Fig. 5a, lane 1). The uracil excision activity in the Ramos B-cell nuclear extracts, which converts dU to an abasic site, was measured as the appearance of an 11-nt cleavage product after incubation for 5 or 10 min (Fig. 5a, lanes 2–13). The cell extract from GANP-overexpressing cells (GANP$^{O/E}$) showed a 1.5-fold increase in UNG-specific activity compared with the control (Fig. 5a, lanes 3, 9). It has been shown that SMUG1 can act as a back-up uracil-DNA glycosylase for dU processing in IgV and S regions during SHM and CSR (40, 41). To differentiate the effect of GANP on UNG and SMUG1 activity, the uracil excision activity of the Ramos extracts was measured in the presence of an anti-SMUG1 neutralizing antibody (Fig. 5a, lanes 5–7, 11–13). Consistent with the low expression of SMUG1 in B cells (40), its inhibition led to only a slight reduction (10–20%) in the UNG activity in each B-cell extract tested (Fig. 5b). The absence of SMUG1 did not alter the effect of GANP on the UNG activity in the Ramos cells. GANP overexpression increased the UNG activity ~1.5-fold and GANP depletion slightly reduced the UNG activity relative to that in the control cells (Fig. 5b). Therefore, GANP may support UNG activity, and the effect of GANP in favoring Ts mutations is mediated through the regulation of the repair mechanism after the UNG-mediated removal of U from single-stranded DNA.

Discussion

Affinity maturation of antibodies occurs after extensive diversification of the immunoglobulin repertoire of B cells. Antibodies with high affinity for a given antigen are generated by cycles of SHM and antigen-affinity selection. This process is similar to the natural evolutionary mechanism, albeit on a much shorter time scale, during which random genomic mutations that confer an advantageous phenotype are selected under survival pressure. However, recent studies suggest the existence of an elaborate

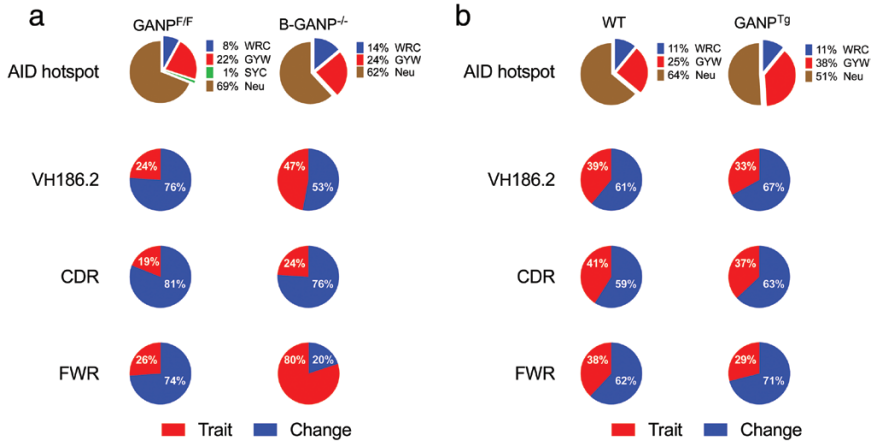

Fig. 4. Hotspot motif preference and patterns of amino acid replacements under the influence of GANP. (a) The GANP$^{F/F}$ and B-GANP$^{-/-}$. (b) WT (continuous line) and GANP^{Tg}. Targeting AID to the WRC hotspot motif (non-transcribed strand) and the GYW hotspot motif (transcribed strand) in B-GANP$^{-/-}$ B cells compared with the GANP$^{F/F}$ B cells, and in GANP^{Tg} B cells compared with WT B cells (upper part of pie charts). Patterns of amino acid replacements in the CDR and FWR of GC B cells (lower part of pie charts). Types of amino acid replacements are represented by pie charts. Red: trait. Blue: change. The pie charts are drawn from the data in Supplementary Table S2 (available at *International Immunology* Online).

mechanism that controls the distribution and types of SHM at the rearranged IgV loci to maximize the affinity maturation and selection of high-affinity memory and plasma B cells (5, 37, 42).

GANP interacts with AID in the cytoplasm and facilitates the translocation of AID to the nucleus and the targeting of AID to the rearranged IgV region (32, 33). In our previous paper, markedly reduced mutations in GANP-IP, probably due to later access of AID after GANP binding, confirms that the role of GANP in the induction of mutation is through AID recruitment, and could mean that mutation profiles observed in GANP-IP are not an accurate reflection of SHM. In our current study, we re-analyzed former mutations to include AID-bound IgV sequences from GFP$^{O/E}$ B cells (Fig. 3a, right panel), as this represents physiological SHM condition. Although GANP is important for generation of high-affinity GC B cells *in vivo* in response to thymus-dependent (TD) antigens (29), its effect on the level of SHM in IgV regions is modest, resulting in increases of <1.5-fold in mice and <2-fold in B-cell lines (Figs 1 and 3; Supplementary Table S1 and Figure S3, available at *International Immunology* Online). The importance of GANP in affinity maturation might be associated with its effect on the distributions and types of IgV-region SHM mutations. The SHM profile is closely associated with the distribution of AID-initiated C→U deaminations on the transcribed and non-transcribed IgV strands and with the downstream processing of U to generate a variety of Ts and Tv mutations at C/G and A/T template sites. The results of this study provide evidence that the mere increase in mutation does not necessarily contribute to increasing the affinity of the IgV region for the target antigens. This might be consistent with the computational statistical analysis with next-generation sequencing of IgV diversification reported by Kleinstein *et al.*, although their study did not mention the relationship with antibody affinity (27, 28). Furthermore, the function of GANP strikingly supports the proposal of Hershberg and Shlomchik (5) that conservative amino acid changes favor the integrity of the antibody, particularly in the FWRs of the IgV structure during affinity maturation. The antibodies generated by the UNG$^{-/-}$ B cells did not significantly lose their affinity for the antigens (43), indicating that SHM with predominant Ts mutations at C/G sites in UNG-negative cells can still generate high-affinity antibodies against TD antigens. This information was clearly presented in early articles (5, 43), but the details have not been examined. The generation of high-affinity antibodies might not solely depend on the extent of diversification in the sequence of overall IgV region.

GANP likely facilitates the access of AID to the non-transcribed strand *in vitro*, as observed by the 9-fold increase in the C:G ratio in endogenous sequences and the 2-fold increase in AID-bound immunoglobulin sequences (32, 33). In the analysis of the IgV-region SHM *in vivo*, GANP reduced the C:G ratio, also implying that GANP controls the AID-induced mutation of the transcribed strand (31). The GANP/AID complex may affect the SHM profile preferentially on the transcribed strand, probably together with the transcriptional machinery. *In vitro*, GANP causes a pause in transcription by recruiting stalling factors (33) and creating a transcription bubble, a structure that facilitates the access of AID to the non-transcribed strand. This may play a role in the MMR mechanism, which has been shown to preferentially target the non-transcribed strand (44). Although UNG and MMR play roles in the further amplification of mutations, the role of GANP might be to restrict the mutation of the IgV region to Ts-biased mutations at the level of MMR and/or the DNA polymerases. However, the regulation of strand preference seems to be a little more complicated *in vivo* than *in vitro*, although our data clearly show that GANP induces a transcription-strand bias.

The codon usage and the amino acid appearance of any given profile are not simply random, but might be inherently regulated to conserve the genotype so that point mutations do not directly cause a functional change. The IgV region, composed of heavy and light chains, forms a pocket that interacts directly with the tertiary structure of an antigen through the loop structures of the CDRs, in which a considerable proportion of

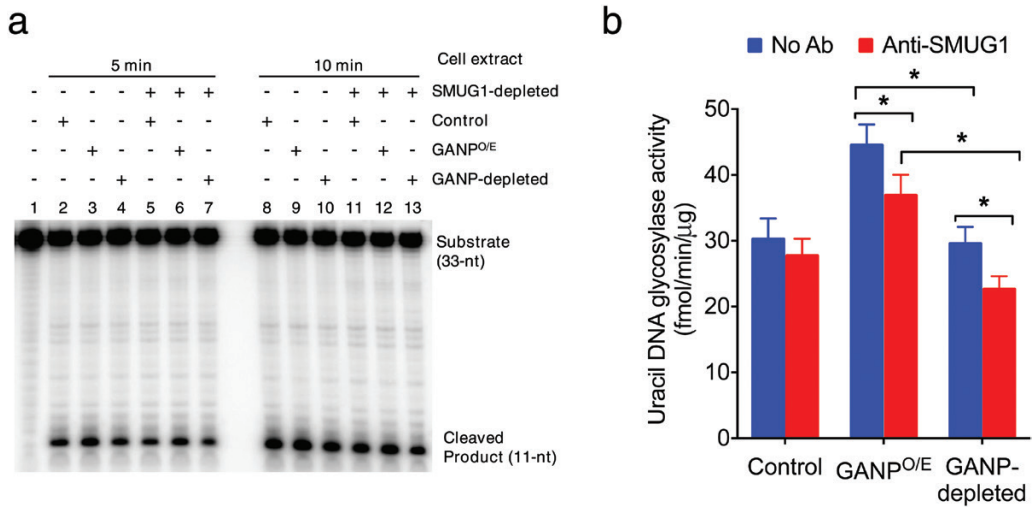

Fig. 5. Effect of GANP overexpression and knockdown on endogenous UNG activity. (a) Uracil excision activity (for an U:G mismatch) in the nuclear extract of Ramos B cells (control), Ramos cells overexpressed with GANP (GANP$^{O/E}$) or GANP knockdown by siRNA (GANP-depleted). ^{32}P-labeled dsDNA (250 fmol) with an U:G mismatch was incubated with 200 ng of nuclear extract for 5 or 10 min. Where indicated, 6 μg of an anti-SMUG1 antibody was incubated with the cell extract to neutralize any SMUG1 activity before the addition of the DNA substrate. Following hot alkali treatment, the 11-nt cleavage product was separated from the 33-nt substrate with 16% denaturing PAGE and visualized with phosphorimaging. (b) UNG activity in Ramos nuclear extracts in the presence or absence of an anti-SMUG1 neutralizing antibody. Specific activity was calculated as femtomole of excised U per minute per microgram of cell extract. Error bars represent the SDs calculated from three independent experiments. *$P < 0.05$.

the amino acid changes is associated with affinity maturation. However, antigen-driven B cells are under pressure to maintain the same antigen specificity, even during the antigen-driven diversification of the IgV repertoire. The conservation of the FWR β-strand is significant for the assembly of the backbone and for the global structure of the IgV region. The CDR loop is highly variable in the genome and the codon usage in the CDRs seems to have developed with a greater inherent tendency to mutate into different amino acids by replacement than the codon usage of the FWRs (5, 37, 45).

A single-nucleotide mutation that will result in an amino acid change was designated an 'amino acid changeability mutation', and changes that cause non-conservative amino acid changes and radically alter the amino acid encoded, including its hydrophobicity, polarity and size, are designated 'trait changeability mutations' (5). Therefore, IgV region SHM profiles appear to be unequal, which is presumably attributable to a Ts bias at the nucleotide level. In our analysis of IgV-region SHM profiles and the affinities of monoclonal antibodies for NP–hapten, the GANP^{Tg} mice favored Ts mutations at C/G, resulting in an amino acid change to a similar or the same amino acid group, classified according to the amino acid properties, particularly in the CDRs. This function may be important for ensuring antigen specificity and the maintenance of the protein backbone in the IgV region during the acquisition of many point mutations at the C nucleotides in the CDRs and FWRs.

As well as BER and MMR, homologous recombination (HR) is also reported to induce SHM (46–49). GANP has been shown to promote HR by suppressing non-homologous end-joining (NHEJ) (39), so HR may be involved in the introduction of single-base substitutions. This would efficiently induce the required amino acid replacement in the IgV region, without disrupting its genomic structure. In contrast, NHEJ roughly reconnects broken ends, which probably induces frameshifts and jeopardizes the whole structure of the IgV region. This could explain why the IgV region must be protected from NHEJ (50). The role of GANP in protecting the IgV genomic structure may be part of a more global role in protecting DNA from damage and is probably associated with transcription-coupled DNA repair.

GANP functions in regulating the access of AID/APOBEC3G to the selected target DNA strand (32, 33, 51). This ability to limit the access of potentially hazardous enzymes is presumably important for protecting the genomes of host cells. Moreover, GANP also minimizes the damage to the genome and presumably prevents the genomic DNA from rigorous alteration by inhibiting NHEJ repair by interacting with and dissociating from the DNA-dependent protein kinase, catalytic subunit (DNA–PKcs) during the DNA damage response (39). Therefore, GANP may play a 'stagehand' role in protecting the protein structure and maintaining the antigen-specific reactivity of the IgV region. GANP is thought to be a crucial molecule that has evolved the AID/APOBEC family of cytidine deaminases in mammals, with their highly developed humoral immunity.

Supplementary data

Supplementary data are available at *International Immunology* Online.

Funding

This work was partly supported by the JSPS KAKENHI (grant number 26460580 to K.M.) and grants from the SENSHIN Medical Research Foundation (to K.M.), the National Institutes of Health (ES13192 and GM21422 to M.F.G) and the Tokyo Metropolitan Institute of Medical Science (to N.S.).

Acknowledgements

We thank Y. Fukushima and E. Kamada for their secretarial assistance and K. Asakawa for technical assistance. We also thank Prof. Hiroyuki Oshiumi (Kumamoto University) for help and cooperation.

Conflicts of Interest statement: The authors declare that they have no competing financial interests.

References

1 Petersen-Mahrt, S. K., Harris, R. S. and Neuberger, M. S. 2002. AID mutates *E. coli* suggesting a DNA deamination mechanism for antibody diversification. *Nature* 418:99.
2 Keim, C., Kazadi, D., Rothschild, G. and Basu, U. 2013. Regulation of AID, the B-cell genome mutator. *Genes Dev.* 27:1.
3 Larijani, M. and Martin, A. 2012. The biochemistry of activation-induced deaminase and its physiological functions. *Semin. Immunol.* 24:255.
4 Wright, B. E., Schmidt, K. H., Hunt, A. T., Reschke, D. K. and Minnick, M. F. 2011. Evolution of coordinated mutagenesis and somatic hypermutation in VH5. *Mol. Immunol.* 49:537.
5 Hershberg, U. and Shlomchik, M. J. 2006. Differences in potential for amino acid change after mutation reveals distinct strategies for kappa and lambda light-chain variation. *Proc. Natl Acad. Sci. USA* 103:15963.
6 Wang, F., Sen, S., Zhang, Y. *et al.* 2013. Somatic hypermutation maintains antibody thermodynamic stability during affinity maturation. *Proc. Natl Acad. Sci. USA* 110:4261.
7 Ramiro, A. R., Stavropoulos, P., Jankovic, M. and Nussenzweig, M. C. 2003. Transcription enhances AID-mediated cytidine deamination by exposing single-stranded DNA on the nontemplate strand. *Nat. Immunol.* 4:452.
8 Kodgire, P., Mukkawar, P., Ratnam, S., Martin, T. E. and Storb, U. 2013. Changes in RNA polymerase II progression influence somatic hypermutation of Ig-related genes by AID. *J. Exp. Med.* 210:1481.
9 Chaudhuri, J., Tian, M., Khuong, C., Chua, K., Pinaud, E. and Alt, F. W. 2003. Transcription-targeted DNA deamination by the AID antibody diversification enzyme. *Nature* 422:726.
10 Basu, U., Meng, F. L., Keim, C. *et al.* 2011. The RNA exosome targets the AID cytidine deaminase to both strands of transcribed duplex DNA substrates. *Cell* 144:353.
11 Rada, C., Di Noia, J. M. and Neuberger, M. S. 2004. Mismatch recognition and uracil excision provide complementary paths to both Ig switching and the A/T-focused phase of somatic mutation. *Mol. Cell* 16:163.
12 Di Noia, J. M., Williams, G. T., Chan, D. T., Buerstedde, J. M., Baldwin, G. S. and Neuberger, M. S. 2007. Dependence of antibody gene diversification on uracil excision. *J. Exp. Med.* 204:3209.
13 Rada, C., Williams, G. T., Nilsen, H., Barnes, D. E., Lindahl, T. and Neuberger, M. S. 2002. Immunoglobulin isotype switching is inhibited and somatic hypermutation perturbed in UNG-deficient mice. *Curr. Biol.* 12:1748.
14 Krijger, P. H., Tsaalbi-Shtylik, A., Wit, N., van den Berk, P. C., de Wind, N. and Jacobs, H. 2013. Rev1 is essential in generating G to C transversions downstream of the Ung2 pathway but not the Msh2+Ung2 hybrid pathway. *Eur. J. Immunol.* 43:2765.
15 Di Noia, J. and Neuberger, M. S. 2002. Altering the pathway of immunoglobulin hypermutation by inhibiting uracil-DNA glycosylase. *Nature* 419:43.
16 Roa, S., Li, Z., Peled, J. U., Zhao, C., Edelmann, W. and Scharff, M. D. 2010. MSH2/MSH6 complex promotes error-free repair of AID-induced dU:G mispairs as well as error-prone hypermutation of A:T sites. *PLoS ONE* 5:e11182.
17 Weill, J. C. and Reynaud, C. A. 2008. DNA polymerases in adaptive immunity. *Nat. Rev. Immunol.* 8:302.
18 Zhao, Y., Gregory, M. T., Biertümpfel, C., Hua, Y. J., Hanaoka, F. and Yang, W. 2013. Mechanism of somatic hypermutation at the WA motif by human DNA polymerase η. *Proc. Natl Acad. Sci. USA* 110:8146.
19 Krijger, P. H., Langerak, P., van den Berk, P. C. and Jacobs, H. 2009. Dependence of nucleotide substitutions on Ung2, Msh2, and PCNA-Ub during somatic hypermutation. *J. Exp. Med.* 206:2603.
20 Shen, H. M., Tanaka, A., Bozek, G., Nicolae, D. and Storb, U. 2006. Somatic hypermutation and class switch recombination in Msh6(-/-)Ung(-/-) double-knockout mice. *J. Immunol.* 177:5386.
21 Maul, R. W., Saribasak, H., Martomo, S. A. *et al.* 2011. Uracil residues dependent on the deaminase AID in immunoglobulin gene variable and switch regions. *Nat. Immunol.* 12:70.
22 Shlomchik, M. J., Marshak-Rothstein, A., Wolfowicz, C. B., Rothstein, T. L. and Weigert, M. G. 1987. The role of clonal selection and somatic mutation in autoimmunity. *Nature* 328:805.
23 Lossos, I. S., Okada, C. Y., Tibshirani, R. *et al.* 2000. Molecular analysis of immunoglobulin genes in diffuse large B-cell lymphomas. *Blood* 95:1797.
24 Boyd, S. D., Marshall, E. L., Merker, J. D. *et al.* 2009. Measurement and clinical monitoring of human lymphocyte clonality by massively parallel VDJ pyrosequencing. *Sci. Transl. Med.* 1:12ra23.
25 Wu, Y. C., Kipling, D., Leong, H. S., Martin, V., Ademokun, A. A. and Dunn-Walters, D. K. 2010. High-throughput immunoglobulin repertoire analysis distinguishes between human IgM memory and switched memory B-cell populations. *Blood* 116:1070.
26 Jiang, N., Weinstein, J. A., Penland, L., White, R. A. 3rd, Fisher, D. S. and Quake, S. R. 2011. Determinism and stochasticity during maturation of the zebrafish antibody repertoire. *Proc. Natl Acad. Sci. USA* 108:5348.
27 Yaari, G., Uduman, M. and Kleinstein, S. H. 2012. Quantifying selection in high-throughput immunoglobulin sequencing data sets. *Nucleic Acids Res.* 40:e134.
28 Uduman, M., Yaari, G., Hershberg, U., Stern, J. A., Shlomchik, M. J. and Kleinstein, S. H. 2011. Detecting selection in immunoglobulin sequences. *Nucleic Acids Res.* 39:W499.
29 Sakaguchi, N., Maeda, K. and Kuwahara, K. 2011. Molecular mechanism of immunoglobulin V-region diversification regulated by transcription and RNA metabolism in antigen-driven B cells. *Scand. J. Immunol.* 73:520.
30 Sakaguchi, N. and Maeda, K. 2016. Germinal center B-cell-associated nuclear protein (GANP) involved in RNA metabolism for B cell maturation. *Adv. Immunol.* 131:135.
31 Sakaguchi, N., Kimura, T., Matsushita, S. *et al.* 2005. Generation of high-affinity antibody against T cell-dependent antigen in the Ganp gene-transgenic mouse. *J. Immunol.* 174:4485.
32 Maeda, K., Singh, S. K., Eda, K. *et al.* 2010. GANP-mediated recruitment of activation-induced cytidine deaminase to cell nuclei and to immunoglobulin variable region DNA. *J. Biol. Chem.* 285:23945.
33 Singh, S. K., Maeda, K., Eid, M. M. *et al.* 2013. GANP regulates recruitment of AID to immunoglobulin variable regions by modulating transcription and nucleosome occupancy. *Nat. Commun.* 4:1830.
34 Garcia-Boronat, M., Diez-Rivero, C. M., Reinherz, E. L. and Reche, P. A. 2008. PVS: a web server for protein sequence variability analysis tuned to facilitate conserved epitope discovery. *Nucleic Acids Res.* 36:W35.
35 Maccarthy, T., Roa, S., Scharff, M. D. and Bergman, A. 2009. SHMTool: a webserver for comparative analysis of somatic hypermutation datasets. *DNA Repair (Amst.)* 8:137.
36 Nilsen, H., Haushalter, K. A., Robins, P., Barnes, D. E., Verdine, G. L. and Lindahl, T. 2001. Excision of deaminated cytosine from the vertebrate genome: role of the SMUG1 uracil-DNA glycosylase. *EMBO J.* 20:4278.
37 Zheng, N. Y., Wilson, K., Jared, M. and Wilson, P. C. 2005. Intricate targeting of immunoglobulin somatic hypermutation maximizes the efficiency of affinity maturation. *J. Exp. Med.* 201:1467.
38 Saribasak, H., Saribasak, N. N., Ipek, F. M., Ellwart, J. W., Arakawa, H. and Buerstedde, J. M. 2006. Uracil DNA glycosylase disruption blocks Ig gene conversion and induces transition mutations. *J. Immunol.* 176:365.
39 Eid, M. M., Maeda, K., Almofty, S. A., Singh, S. K., Shimoda, M. and Sakaguchi, N. 2014. GANP regulates the choice of DNA repair pathway by DNA-PKcs interaction in AID-dependent IgV region diversification. *J. Immunol.* 192:5529.

40 Di Noia, J. M., Rada, C. and Neuberger, M. S. 2006. SMUG1 is able to excise uracil from immunoglobulin genes: insight into mutation versus repair. *EMBO J.* 25:585.
41 Dingler, F. A., Kemmerich, K., Neuberger, M. S. and Rada, C. 2014. Uracil excision by endogenous SMUG1 glycosylase promotes efficient Ig class switching and impacts on A:T substitutions during somatic mutation. *Eur. J. Immunol.* 44:1925.
42 Liu, M. and Schatz, D. G. 2009. Balancing AID and DNA repair during somatic hypermutation. *Trends Immunol.* 30:173.
43 Zahn, A., Daugan, M., Safavi, S. *et al.* 2013. Separation of function between isotype switching and affinity maturation *in vivo* during acute immune responses and circulating autoantibodies in UNG-deficient mice. *J. Immunol.* 190:5949.
44 Unniraman, S. and Schatz, D. G. 2007. Strand-biased spreading of mutations during somatic hypermutation. *Science* 317:1227.
45 Sun, S. B., Sen, S., Kim, N. J., Magliery, T. J., Schultz, P. G. and Wang, F. 2013. Mutational analysis of 48G7 reveals that somatic hypermutation affects both antibody stability and binding affinity. *J. Am. Chem. Soc.* 135:9980.
46 Papavasiliou, F. N. and Schatz, D. G. 2000. Cell-cycle-regulated DNA double-stranded breaks in somatic hypermutation of immunoglobulin genes. *Nature* 408:216.
47 Zan, H., Wu, X., Komori, A., Holloman, W. K. and Casali, P. 2003. AID-dependent generation of resected double-strand DNA breaks and recruitment of Rad52/Rad51 in somatic hypermutation. *Immunity* 18:727.
48 Bross, L., Wesoly, J., Buerstedde, J. M., Kanaar, R. and Jacobs, H. 2003. Somatic hypermutation does not require Rad54 and Rad54B-mediated homologous recombination. *Eur. J. Immunol.* 33:352.
49 Li, Z., Woo, C. J., Iglesias-Ussel, M. D., Ronai, D. and Scharff, M. D. 2004. The generation of antibody diversity through somatic hypermutation and class switch recombination. *Genes Dev.* 18:1.
50 Bastianello, G. and Arakawa, H. 2017. A double-strand break can trigger immunoglobulin gene conversion. *Nucleic Acids Res.* 45:231.
51 Maeda, K., Almofty, S. A., Singh, S. K. *et al.* 2013. GANP interacts with APOBEC3G and facilitates its encapsidation into the virions to reduce HIV-1 infectivity. *J. Immunol.* 191:6030.